Received: 6 June 2021 | Revised: 25 October 2021 | Accepted: 26 October 2021

DOI: 10.1111/cas.15184

ORIGINAL ARTICLE

Cancer Science WILEY

SNHG17, as an EMT-related lncRNA, promotes the expression of c-Myc by binding to c-Jun in esophageal squamous cell carcinoma

Supeng Shen[1] | Jia Liang[1] | Xiaoliang Liang[2] | Gaoyan Wang[1] | Bo Feng[2] | Wei Guo[2] | Yanli Guo[1] | Zhiming Dong[1]

[1]the Fourth Hospital of Hebei Medical University, Shijiazhuang, China

[2]Laboratory of Pathology, Hebei Cancer Institute, the Fourth Hospital of Hebei Medical University, Shijiazhuang, China

Correspondence
Zhiming Dong, Biobank, the Fourth Hospital of Hebei Medical University, Shijiazhuang, China.
Email: dongzhiming2001@163.com

Funding information
Natural Science Foundation of Hebei Province, China, Grant/Award Number: H2019206664; This study was supported by Grants from the National Natural Science Foundation, Grant/Award Number: 81472335 and 81772612

Abstract

Dysregulation of long noncoding RNA *SNHG17* is associated with the occurrence of several tumors; however, its role in esophageal squamous cell carcinoma (ESCC) remains obscure. The present study demonstrated that *SNHG17* was upregulated in ESCC tissues and cell lines, induced by TGF-β1, and associated with poor survival. It is also involved in the epithelial-to-mesenchymal transition (EMT) process. The mechanism underlying *SNHG17*-regulated c-Myc was detected by RNA immunoprecipitation, RNA pull-down, chromatin immunoprecipitation, and luciferase reporter assays. *SNHG17* was found to directly regulate c-Myc transcription by binding to c-Jun protein and recruiting the complex to specific sequences of the c-*Myc* promoter region, thereby increasing its expression. Moreover, *SNHG17* hyperactivation induced by TGF-β1 results in PI3K/AKT pathway activation, promoting cells EMT, forming a positive feedback loop. Furthermore, *SNHG17* facilitated ESCC tumor growth in vivo. Overall, this study demonstrated that the *SNHG17*/c-Jun/c-Myc axis aggravates ESCC progression and EMT induction by TGF-β1 and may serve as a new therapeutic target for ESCC.

KEYWORDS

c-Myc, EMT, esophageal squamous cell carcinoma, metastasis, *SNHG17*

1 | INTRODUCTION

Esophageal cancer is one of the most common gastrointestinal tumors worldwide, ranking seventh in incidence and sixth in cancer-related mortality in 2018.[1] The main types of esophageal cancers are ESCC and esophageal adenocarcinoma (EAC).[2] ESCC is the predominant histological type of esophageal cancer in China.[3] The geographical variation in the incidence is striking, exhibiting a high prevalence in the Taihang mountain region in north-central China, such as Cixian in Hebei, Henan, and Shanxi provinces.[4] Although there have been great advances in the treatment of esophageal cancer, patients with ESCC experience malignant proliferation and invasion, leading to poor survival (5-y survival rate <30%).[5,6] Therefore, understanding the ESCC progression mechanism to improve the clinical outcome of patients with ESCC is essential.

Abbreviations: ChIP, chromatin immunoprecipitation; DEG, differentially expressed gene; EMT, epithelial-to-mesenchymal transition; ESCC, esophageal squamous cell carcinoma; GEO, Gene Expression Omnibus; GEPIA, Gene Expression Profiling Interactive Analysis; ISH, in situ hybridization; lncRNA, long noncoding RNA; OS, overall survival; RIP, RNA-binding protein immunoprecipitation; *SNHG17*, small nucleolar RNA host gene 17; TGF-β1, transforming growth factor-β1.

Long noncoding RNAs (lncRNAs) are RNA molecules with length exceeding 200 nucleotides (nt) and account for >76% of noncoding RNAs (ncRNAs).[7,8] The lncRNAs have been implicated in a wide repertoire of cellular processes, including cell differentiation, cell cycle regulation, cell apoptosis, and epithelial-to-mesenchymal transition (EMT).[9,10] Recent studies have shown that lncRNAs serve as master regulators in tumor progression and play a key role in encouraging or combating carcinogenesis, including ESCC.[11,12] The oncogenic role of a lncRNA, small nucleolar RNA host gene 17 (*SNHG17*), has been reported, in which it annotates cancer-associated lncRNA functionally and is mechanistically linked to disease pathogenesis in colon cancer,[13] prostate cancer,[14] gastric cancer,[15] and non–small-cell lung cancer.[16] *SNHG17* acts as a prognostic factor, promoting tumor proliferation and metastasis and is related to poor prognosis in these cancers. Nonetheless, how *SNHG17* participates in the progress of ESCC is yet unknown.

EMT is a cellular process that regulates cancer cell invasion, metastatic potential, and resistance to radiation and chemotherapy. TGF-β acts as a potent EMT-inducing cytokine in promoting cancer cell invasion and metastasis.[17] Moreover, TGF-β-induced lncRNAs have been shown to play crucial roles in various carcinogenic processes. For instance, long noncoding RNA activated by transforming growth factor-beta (lncRNA-ATB) may be induced by TGF-β treatment to facilitate the malignant progression of hepatocellular carcinoma and breast cancer cells.[18,19] TGF-β-activated lncRNA UCA1 promotes the proliferation of bladder transitional carcinoma cells through the non-canonical PI3K-AKT pathway.[20] In prostate cancer, knockdown of *SNHG17* weakened the EMT progression of cancer cells.[14] Together, these studies suggested that lncRNA plays a major role in TGF-β-induced tumor invasion and metastasis. However, few studies have addressed the mechanism of interaction between lncRNA and TGF-β classical and non-classical pathways in ESCC. Additionally, *SNHG17* promotes tumor invasion and metastasis in oral squamous cell carcinoma,[21] gastric cancer,[22] and other gastrointestinal tumors.[23] Therefore, we speculated that *SNHG17* is related to TGF-β ESCC; and whether TGF-β-regulated *SNHG17* is involved in EMT needs further exploration.

In the current study, we aimed to investigate the biological function of *SNHG17* and its role in TGF-β1-induced EMT in ESCC. Therefore, we unveiled the molecular mechanism underlying the pathogenesis of ESCC. These findings indicated that *SNHG17* acts as a potential therapeutic strategy for ESCC.

2 | MATERIALS AND METHODS

2.1 | Microarray data analysis

The human microarray dataset (GSE20347) was downloaded from the public GEO database (http://www.ncbi.nlm.nih.gov/geo). Primary tumor samples (17 ESCC patients from a high-risk region of China) were used to analyze these datasets. The DEGs were screened out with a cut-off value of $P < .05$ and $\log_2$ (fold change) > 2. For RNA-sequencing, total RNA was obtained from Eca109 cells transfected with *sh-SNHG17* or *sh-NC* and subjected to sequencing.

2.2 | Human ESCC tissue specimens

In total, 128 matched ESCC and paired para-cancerous tissues (at least 5 cm distal to tumor lesion) were collected from the Fourth Affiliated Hospital of Hebei Medical University, Shijiazhuang, China from May 2012 to December 2015. Clinical and survival data of patients were provided by the clinical data registry (Table S1). Ethical approval for this study was obtained from the Ethics Committee of the Fourth Affiliated Hospital, Hebei Medical University.

2.3 | Cell culture

Human ESCC cell lines (TE1, Eca109, Kyse150, Kyse170, and Yes2) were purchased from the American Type Culture Collection and maintained in RPMI-1640 medium (Invitrogen) supplemented with 10% fetal bovine serum (Invitrogen). When cells reached 70%-80% confluency, cells were stimulated with 10 ng/mL recombinant TGF-β1 (R&D Systems Inc) for 7 d. Then, total RNA was extracted and reverse transcribed into cDNA to examine *SNHG17* expression.

2.4 | Quantitative real-time polymerase chain reaction (qRT-PCR) analysis

Total RNA was extracted from ESCC tissues and cells using TRIzol reagent (Invitrogen). Then, 1 μg of the total RNA was reverse transcribed into cDNA as detailed by the manufacture (Roche). Quantitative real-time PCR assay was performed using the SYBR qPCR Master Mix (Life Technology). Relative expression levels of lncRNA/mRNA were normalized to that of the housekeeping gene *β-actin* and quantitated by the comparative cycle threshold (C_t) method ($2^{-\Delta\Delta Ct}$). Primers sequences and reaction assays for this study are displayed in Table S2.

2.5 | Plasmid construction and cell transfection

Gene-specific shRNAs targeting *SNHG17*, control shRNAs, small interfering RNAs (siRNAs) targeting c-Jun, and *siNC* were synthesized by GenePharma Company. Overexpression plasmids containing pcDNA3.1-SNHG17 and pcDNA3.1-c-Jun, were synthesized by Genscript Company. SNHG17-MUT (Δ101-400 bp truncated mutant) overexpression vector was purchased from GenePharma. To construct expression vectors for His-tagged c-Jun, cDNAs encoding c-Jun or truncated versions (Δ1-242AA, Δ243-331AA) of c-Jun were synthesized by Generay and subcloned into the *Nde*I and *Xho*I sites of the pET-28a-His vector. The c-*Myc* promoter region (−998 to +73bp) and a truncation (c-Myc-P1 containing binding sites E1 and E2, −335 to +73 bp) were cloned into the pGL3-basic vector, and named c-Myc-wild type (WT) and c-Myc-P1, respectively. Point mutations of c-Jun binding to pGL3-c-Myc-WT were promoted using a Q5® Site-Directed Mutagenesis Kit (New England Biolabs), and named c-Myc-MUT.

Lipofectamine 2000 (Invitrogen) was used to transfect Eca109 or Kyse150 cells inoculated into six-well plates and transfected, respectively, with plasmids or siRNA for 24 h. All sequences are shown in Table S3.

2.6 | Cell proliferation

MTS and colony forming assays were performed to determine the ability for cellular proliferation. For MTS assay, Eca109, Kyse150, and TE1 cells transfected with pcDNA3.1-SNHG17/shSNHG17 were seeded into 96-well plates. After 0, 24, 48, 72, or 96 h of incubation, assays were performed by adding 20 μL of the CellTiter 96®AQ_{ueous} One Solution Reagent (Promega) directly to the culture wells, followed by incubation at 37°C for 4 h. Absorbance was recorded at 490 nm on a microplate reader (Thermo Fisher Scientific).

For the colony forming assay, Eca109, Kyse150 and TE1 cells were seeded into six-well plates at a density of 3000-5000 cells/well and cultured for 7 d. The surviving colonies were fixed in 4% paraformaldehyde and stained with 0.4% crystal violet solution and counted.

2.7 | Flow cytometry cell apoptosis assays

Eca109 and Kyse150 cells transfected with *shSNHG17* were collected after 48 h and washed with PBS. Then, the cells were resuspended in 1× binding buffer at a concentration of 1×10^6 cells/mL. After double staining with 5 μL fluorescein isothiocyanate (PE)-annexin V and 5 μL 7-amino-actinomycin (7-AAD; BD Pharmingen™), the cells were analyzed on a flow cytometer.

2.8 | Migration and invasion assays

For the cell migration assay, 1×10^5 infected Eca109, Kyse150 or TE1 cells were plated on non-Matrigel-coated in the upper chamber (Corning Company) with 200 μL of serum-free medium, and 600 μL of RPMI-1640 medium containing 20% serum was placed in the lower chamber. For the invasion assay, cells were seeded onto 50 μL 1× Matrigel® Basement Membrane Matrix (BD Biosciences)-coated chambers. The culture plate was incubated for 24 h, followed by staining with 0.1% crystal violet and counted under a light microscope.

2.9 | Western blot analysis

Total protein extracts were separated using 10% SDS-PAGE and transferred to PVDF membranes (Millipore). Then, the membranes were blocked with 5% skimmed milk and probed overnight at 4°C with specific primary antibodies, followed by incubation with anti-rabbit IgG antibody (dilution ratio of 1:1000; 075-1506, SeeBio Biotechnology Company). The diluted primary antibodies for our study were as follows: c-Myc (E-AB-62131, Elabscience), AKT (E-AB-30465, Elabscience), p-AKT (E-AB-20802, Elabscience).

2.10 | ISH and immunohistochemistry (IHC)

The same paraffin-embedded sample was serially sectioned, one for ISH, the other IHC staining. Detection of *SNHG17* in ESCC was performed using the SNHG17 ISH Kit (BOSTER Biological Technology Co. Ltd, MK10905-h) according to the protocol provided by the manufacturer. Briefly, paraffin-embedded slides were de-paraffinized by immersion in xylene (10 min twice) and then rehydrated through serial ethanol (100%, 95%, 80%, and 70%) for 5 min each followed by immersion in DEPC-treated PBS for 5 min. Then slides were incubated with pepsin for 20 min at 37°C and hybridized with the *SNHG17* probe (200 nM) overnight at 37°C. The samples were incubated with blocking solution for 30 min, anti-digoxigenin (anti-DIG) reagent was applied for 60 min, and the probe signal was visualized with diaminobenzidine (DAB) solution (BOSTER).

IHC assay was performed as described previously.[24] The paraffin-embedded sections were dewaxed and hydrated in a xylene bath and absolute ethanol solution. Primary antibodies used for the study were as follows: c-Myc (ab32795), Ki-67(bs-23103R). The ISH and IHC results were evaluated as follows: 0 (no staining, no positive cells), 1 (1%-25% positive cells), 2 (26%-50% positive), 3 (51%-75% positive) and 4 (>75% positive). Tissues with scores of 3 and 4 were classified as high expression, and those with scores of 0, 1, and 2 were deemed low expression. To eliminate the subjective evaluation error of percentage, ImageJ software (National Institutes of Health, USA) was used to score signals for inconsistencies in the percentages of the IHC and ISH signals.

2.11 | Isolation of cytoplasmic/nuclear RNA

The nuclear and cytoplasmic fractions of Eca109 and Kyse150 cells were isolated according to the protocol of the PARIS™ Kit Protein and RNA Isolation System (Invitrogen). Total RNA was isolated simultaneously from independent cytoplasmic and nuclear fractions. Finally, qRT-PCR was used to determine the relative expression of *SNHG17* to estimate the relative ratios of *SNHG17* in nuclear and cytoplasmic RNA concentrations.

2.12 | RNA-binding protein immunoprecipitation assay (RIP)

RIP was performed for Eca109 and Kyse150 cells using the Magna RIP™ RNA-Binding Protein Immunoprecipitation Kit (Millipore). Eca109 and Kyse150 cells were lysed in complete RIP lysis buffer (Millipore). The lysates were incubated with magnetic beads (Millipore) conjugated to anti-c-Jun antibody (Cell Signaling Technology) and control IgG antibody. Finally, total RNA was extracted for subsequent qRT-PCR analysis.

2.13 | RNA pull-down assay

Biotin-labeled RNA pull-down assays were performed on Eca109 cells as instructed by the supplier for Pierce™ Magnetic RNA-Protein Pull-Down Kit (Thermo Fisher Scientific). *SNHG17* and antisense-*SNHG17* were transcribed in vitro from linearized constructs using the RiboMAX™ Large-Scale RNA Production Systems (Promega). Streptavidin magnetic beads (Promega) were applied to isolate the RNA-binding protein complexes. Finally, proteins were detected by western blot assay.

2.14 | Chromatin immunoprecipitation (ChIP)

ChIP assay was conducted in Eca109 cells. Cross-linked chromatin DNA was sheared into fragments (200-1000 bp) using ultrasound, and immunoprecipitated with anti-c-Jun (Cell Signaling Technology). After washing the beads, purified DNA was isolated for qRT-PCR.

2.15 | Luciferase reporter assay

Different sequences of the c-*Myc* promoter region (−1000 bp to transcription start site [TSS]) containing or lacking a c-Jun-binding element were added into the pGL3-basic vector (Promega). Eca109 cells were transfected with pGL3-c-Myc (−998 to +73) or pGL3-Myc (−335 to +73) plasmids. Luciferase activity was assessed after 48 h using a Dual-Luciferase Reporter Assay System (Promega). *Renilla* luciferase was used for normalization.

2.16 | Tumor formation assay

Here, G-418 bioreagent (Merck Co., Ltd) was used to generate stable Eca109 cells transfected with pcDNA3.1SNHG17 or empty vector. Here, 100 μL of the cell suspension (1 × 107 cells/mL) were subcutaneously injected into 1 side of BALB/nu nude mice (aged 4-6 wk; Beijing HFK Bioscience Co., Ltd). Tumor formation was examined every 4 d and the tumor volumes calculated. The mice were dissected after 30 d, and tumors were excised from mice for weight assessment. Animal experiments were approved by the Committee on the Ethics of Animal Experiments of the Fourth Affiliated Hospital of Hebei Medical University.

2.17 | Statistical analysis

All statistical analyses were performed using the SPSS 22.0 software. Student *t* test or paired Student *t* test was conducted to compare between the 2 groups. Chi-square (χ^2) test was applied to analyze the association between *SNHG17* expression and clinicopathological features. All experiments data were presented as mean ± SD from 3 independent experiments performed in duplicate. $P < .05$ indicated statistical significance.

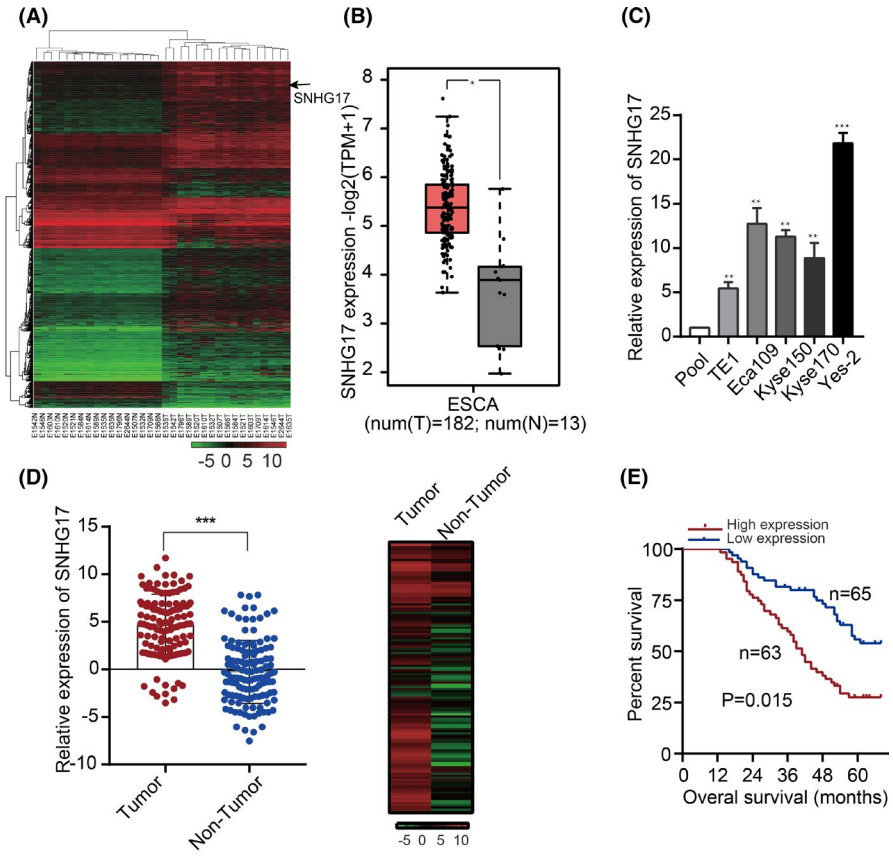

FIGURE 1 *SNHG17* is elevated in ESCC tissues and cell lines and associated with a poor prognosis. A, GEO database (GSE20347) analysis showed the expression of *SNHG17* in 17 ESCC tissues and matched para-tumorous tissues. B, Expression level of *SNHG17* in 182 ESCA tumor samples and 13 normal controls from TCGA database. C, Expression of *SNHG17* in ESCC cell lines and pools, as shown by qRT-PCR. Pools: average expression in 10 normal tissues was used as the normal control. D, Expression of *SNHG17* in ESCC tissues and matched para-normal tissues was detected by qRT-PCR. Heatmap shows the expression of *SNHG17* in each pair of samples. E, Kaplan-Meier curves of *SNHG17* in ESCC patients for OS. Error bars are shown as mean ± SD. *$P < .05$, **$P < .01$, ***$P < .001$

TABLE 1 Correlation of the expression level of *SNHG17* with clinicopathologic features of ESCC patients

Characteristics	N	*SNHG17* expression		*P*-value
		Low n (%)	High n (%)	
Age (y)				
<58	59	32 (54.29)	27 (45.76)	.470
≥58	69	33 (47.83)	36 (52.17)	
Gender				
Male	72	39 (54.17)	33 (45.83)	.385
Female	56	26 (46.43)	30 (53.57)	
TNM stage				
I	14	12 (85.71)	2 (14.29)	<.001***
II	42	34 (80.95)	8 (19.05)	
III	57	14 (24.56)	43 (75.44)	
IV	15	5 (33.33)	10 (66.67)	
Depth of invasion				
T1	17	14 (82.35)	3 (17.65)	<.001***
T2	19	16 (84.21)	3 (15.79)	
T3	78	31 (39.74)	47 (60.26)	
T4	14	4 (28.57)	10 (71.43)	
Pathological differentiation				
Well/moderate	102	57 (55.88)	45 (44.12)	.022*
Poor	26	8 (30.77)	18 (69.23)	
Lymph node metastasis				
Negative (N0)	63	41 (65.08)	22 (34.92)	.01*
Positive (N1/2/3)	65	24 (36.92)	41 (63.08)	
Distant metastasis				
Negative	102	51 (50.00)	51 (50.00)	.726
Positive	26	14(53.85)	12 (46.15)	
Family history of upper gastrointestinal cancer				
Negative	99	52 (52.53)	47 (47.47)	.466
Positive	29	13 (44.83)	16 (55.17)	
Mortality				
Survive	57	36 (63.16)	21 (36.84)	.012*
Die	71	29 (40.85)	42 (59.15)	

*$P < .05$; **$P < .01$; ***$P < .001$.

TABLE 2 Univariate and multivariate Cox regression analysis for clinicopathological features associated with prognosis of 128 ESCC patients

Variables	Univariate analysis		Multivariate analysis	
	HR (95% CI)	*P*	HR (95% CI)	*P*
Age (<58 vs ≥58)	1.040 (0.654-1.656)	.867	0.984 (0.601-1.612)	.950
Gender (male vs female)	1.285 (0.800-2.065)	.299	1.190 (0.718-1.973)	.183
Lymph node metastasis (negative vs positive)	1.961 (1.226-3.138)	.005**	1.796 (1.060-3.044)	.030*
Distant metastasis or recurrence (negative vs positive)	2.243 (1.075-0.931)	.031*	2.573 (1.144-5.784)	.022*
Pathological differentiation (well/moderate vs poor)	1.303 (0.765-2.245)	.341	1.532 (0.829-2.834)	.174
Depth of invasion (T1/2 vs T3/4)	1.226 (0.732-2.055)	.439	0.647 (0.331-1.265)	.203
TNM stage (I + II vs III + IV)	2.352 (1.412-3.917)	.001**	1.998 (1.026-3.890)	.042*
Family history of upper gastrointestinal cancer (negative vs positive)	1.158 (0.679-1.975)	.590	1.496 (0.796-2.812)	.211
SNHG17 (high vs low)	2.355 (1.456-3.809)	<.001***	1.925 (1.011-3.668)	.046*

*$P < .05$; **$P < .01$; ***$P < .001$.

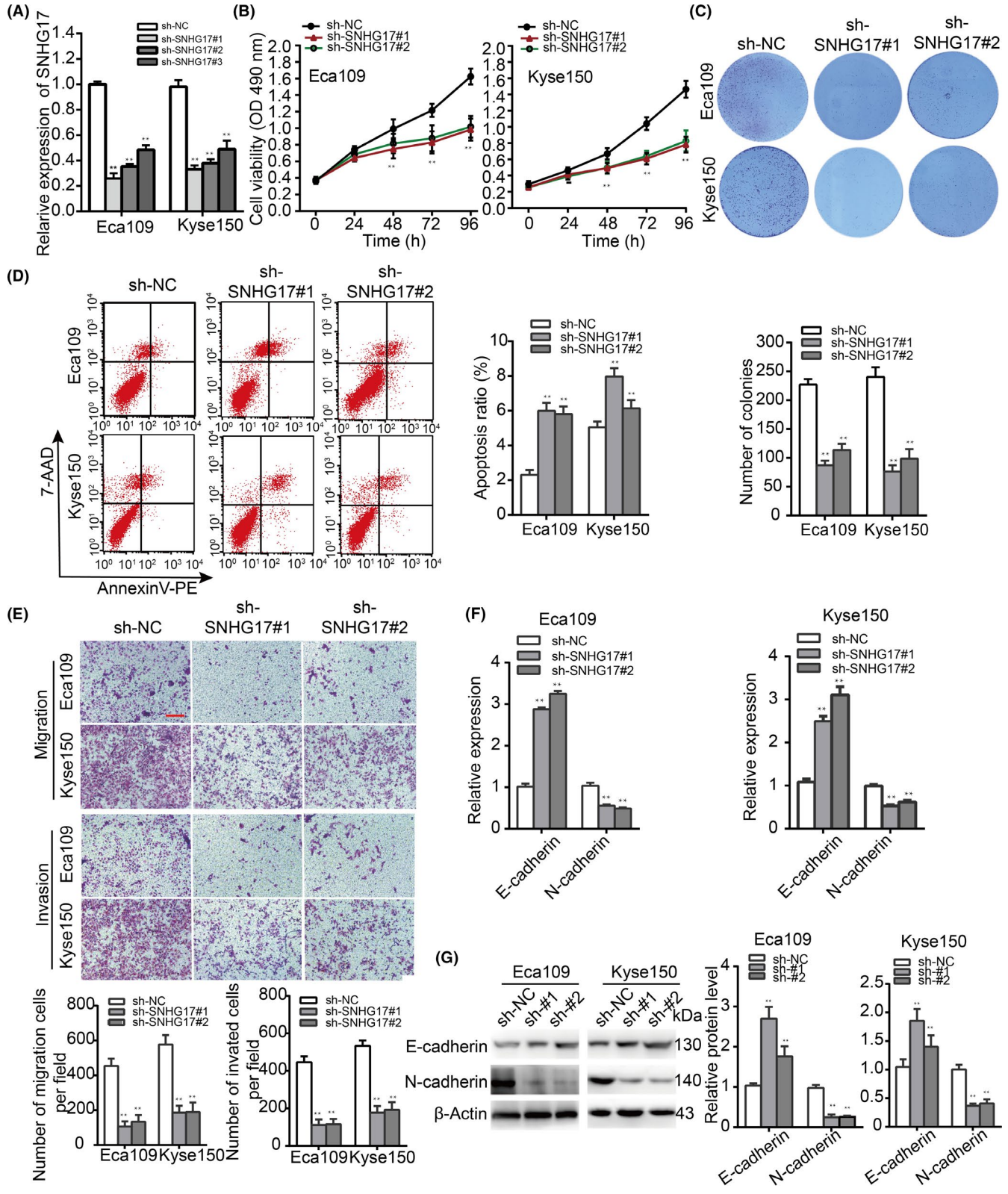

FIGURE 2 *SNHG17* boosts the proliferation, lessens apoptosis, and elevates migration, invasion, and EMT of ESCC cells in vitro. A, Expression of *SNHG17* was detected by qRT-PCR after transfection with *shSNHG17* for 48 h in Eca109 and Kyse150 cells. B, C, MTS and colony forming assays were performed to evaluate Eca109 and Kyse150 cell proliferation after knocking down *SNHG17*. D, Apoptosis of ESCC cells was determined by flow cytometry apoptosis analysis under *SNHG17* knockdown. E, Cell migration and invasion ability were analyzed by transwell assays (magnification: ×100). F, G, qRT-PCR and western blot were performed to examine the expression levels of E-cadherin and N-cadherin in ESCC cells. Error bars are shown as mean ± SD, $^{**}P < .01$

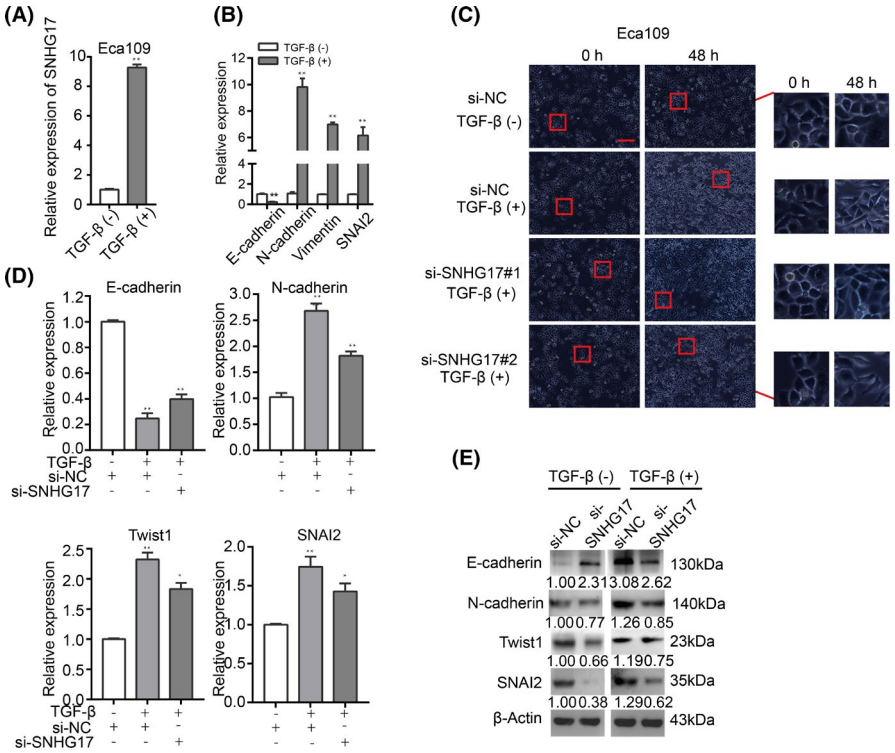

FIGURE 3 *SNHG17* is upregulated in TGF-β-induced Eca109 cells and involved in TGF-β1-mediated EMT. A, Expression of *SNHG17* was assessed in Eca109 treatment with TGF-β1. B, The hallmarks of EMT were detected in TGF-β1-treated Eca109 cells. C, Eca109 cells were transfected with *siNC* and *siSNHG17* for 24 h. Then, cells were transfected again and treated without or with 10 ng/mL TGF-β at 6 h after transfection. Images were acquired at 48 h after the treatment, and representative images of spindle-like shape cells are shown. Red square areas are magnified in the right panel. D, E, Eca109 cells were transfected with *siNC* and *siSNHG17* for 24 h. The cells were then transfected again and treated without or with 10 ng/mL TGF-β1 at 6 h after transfection. At 48 h after treatment, qRT-PCR, and western blot assessed the mRNA and protein expression of EMT-related markers, respectively. Data are presented as mean ± SD. $^{**}P < .01$

3 | RESULTS

3.1 | *SNHG17* is elevated in ESCC tissues and cell lines and associated with a poor prognosis

Based on searches of GEO datasets (GSE20347) and GEPIA (http://gepia2.cancer-pku.cn/#index), the analysis showed that *SNHG17* was markedly upregulated in esophagus cancer samples (Figure 1A,B). For further analysis, primers were designed for different transcript variants of *SNHG17* to identify the transcript of *SNHG17* that boosted the expression of *SNHG17* in ESCC cell lines. Transcript 7 (954 nt long, NR_152757.1) was expressed highly in 5 ESCC cell lines compared with a panel of human esophageal cancer cell lines (Figures 1C and S1). Moreover, 128 pairs of ESCC and adjacent normal tissues were evaluated. Patients were divided into 2 groups based on the median value: high *SNHG17* expression (fold change ≥ median, n = 63) and low *SNHG17* expression (fold change ≤ median, n = 65) groups. As shown in Figure 1D, *SNHG17* expression in cancer tissues was higher than that in the adjacent normal tissues. Upregulated *SNHG17* expression was related to TNM stage, depth of invasion, tumor differentiation, lymph node metastasis, and mortality (Table 1). Additionally, Kaplan-Meier survival analysis indicated that patients with highly expressed *SNHG17* had a significantly poor overall survival (Figure 1E). Univariate and multivariate Cox regression analyses demonstrated that upregulated *SNHG17* was an independent prognostic marker for ESCC patients (Table 2).

3.2 | *SNHG17* boosts the proliferation, lessens apoptosis, and elevates migration, invasion, and EMT of ESCC cells

To address the biological functions of *SNHG17* in ESCC cell lines, we transfected Eca109, Kyse150, and TE1 cells with *shSNHG17* or overexpression vector. The transfection efficiency of *SNHG17* was measured by qRT-PCR. As demonstrated in Figures 2A and S2, the expression of *SNHG17* was significantly decreased by shSNHG17#1/2 and markedly increased by the overexpression vector compared with the control groups. MTS and colony formation assays showed that the downregulated *SNHG17* significantly attenuated cell viability and colony generation compared with the control group (Figure 2B,C). Moreover, flow cytometry cell apoptosis analysis indicated that depletion of *SNHG17* increased the apoptosis of ESCC cells (Figure 2D). Transwell assay demonstrated that the migratory and invasive abilities of Eca109 and Kyse150 cells were drastically weakened after *shSNHG17* transfection (Figure 2E). Conversely, overexpression of *SNHG17* notably increased the proliferation, migration, and invasion of TE1, Eca109 and Kyse150 cells

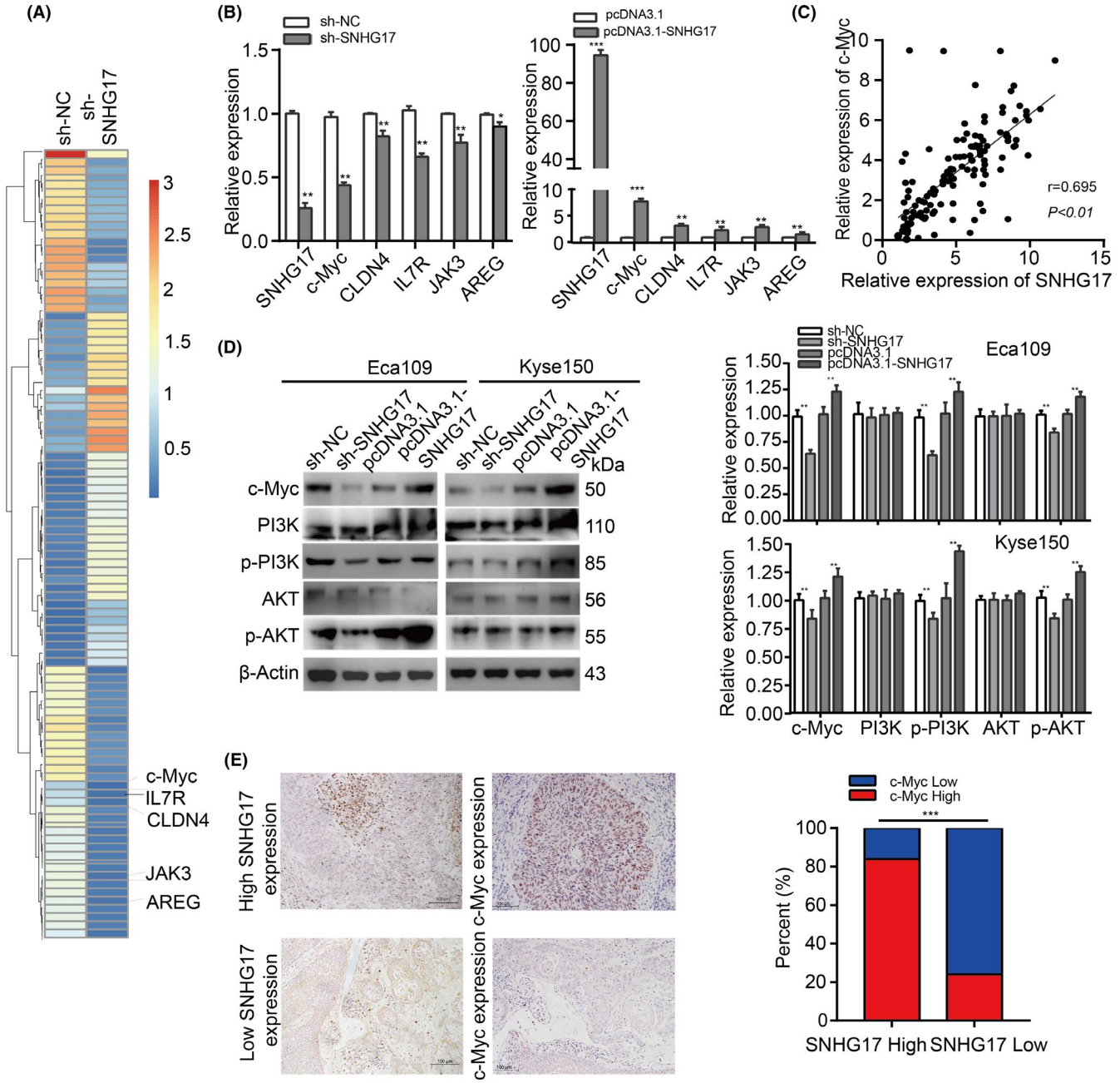

FIGURE 4 *SNHG17* upregulates the expression of c-Myc and medicates the PI3K/AKT pathway in ESCC. A, Hierarchically clustered heatmap of upregulated and downregulated genes in Eca109 cells after transfection with *sh-SNHG17* or *sh-NC*. B, Expression levels of c-*Myc*, *CLDN4*, *IL7R*, *JAK3*, and *AREG* under *SNHG17* silencing or overexpression were identified by qRT-PCR. C, Association analysis of the correlation between c-*Myc* and *SNHG17* expression ($r = .695$, $P < .01$). D, Protein expression of c-Myc, pPI3K, PI3K, p-AKT, and AKT under *SNHG17* knockdown or overexpression, as detected by western blot. E, ISH and IHC staining results showed that the expression of c-Myc was high in the same ESCC paraffin-embedded sample with high *SNHG17* expression, and vice versa. Data are presented as mean ± SD. $^{**}P < .01$

compared with vector-transfected cells (Figure S2). Additionally, qRT-PCR and western blot were performed to examine the EMT-related markers. The results exhibited that the level of E-cadherin expression was dramatically increased, while N-cadherin expression was significantly reduced in *SNHG17*-deficient Eca109 and Kyse150 cells (Figure 2F,G). These findings suggested that high expression of *SNHG17* has a crucial role in facilitating the progression of ESCC.

3.3 | *SNHG17* is upregulated in TGF-β-induced Eca109 cells and involved in TGF-β1-mediated EMT

EMT is a key player in promoting cancer cell migration and invasion.[25] Moreover, since TGF-β1 is required for EMT, we further estimated whether *SNHG17* regulates the migration and invasion of ESCC cells via TGF-β1-mediated EMT. Strikingly, *SNHG17* increased

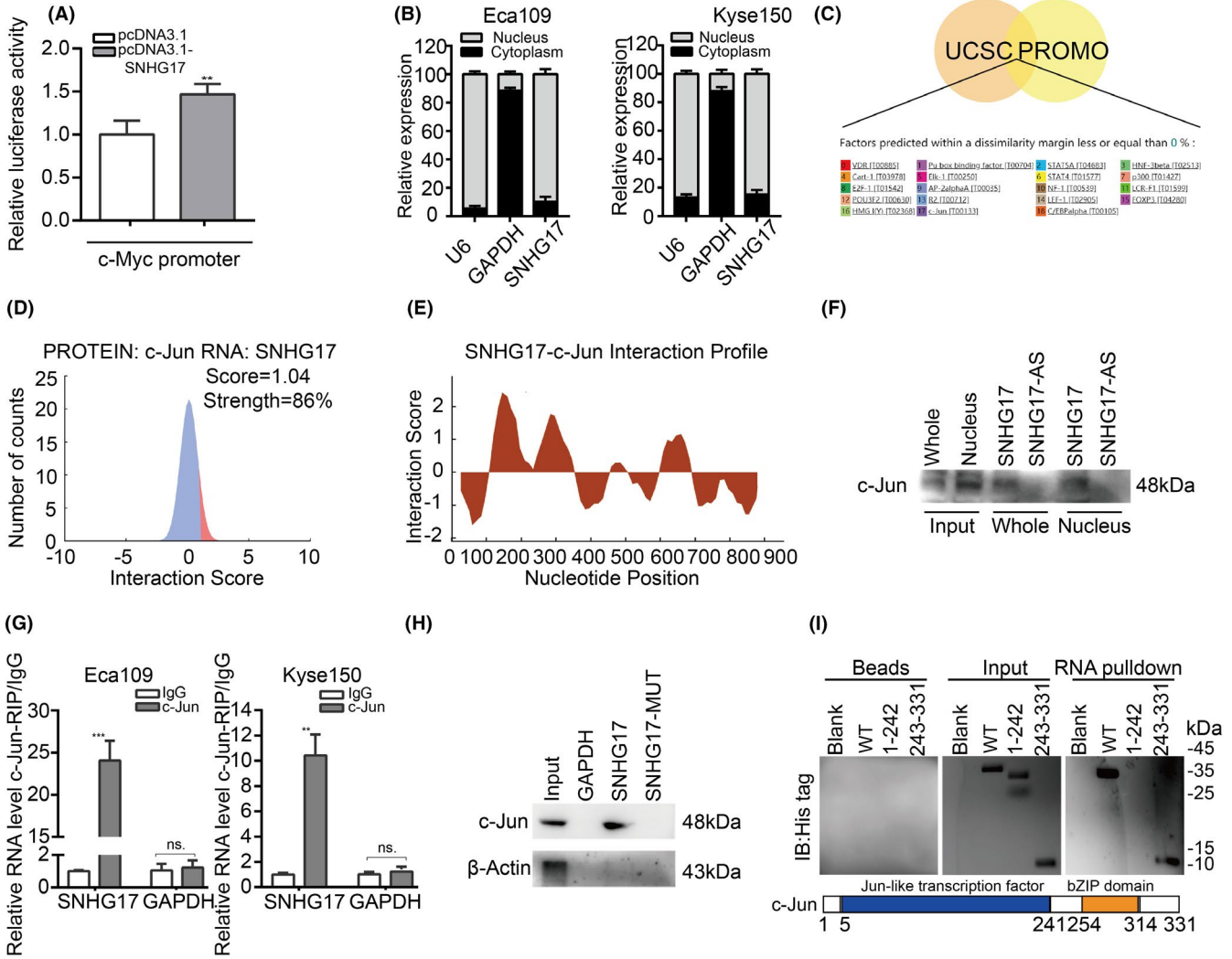

FIGURE 5 *SNHG17* binds to transcription factor c-Jun. A, Luciferase reporter assay suggested that *SNHG17* regulates the transcription of c-Myc. B, Subcellular localization of *SNHG17* in Eca109 and Kyse150 cells. *U6* and *GAPDH* were used as positive controls for nuclear RNA and cytoplasmic RNA, respectively. C, TFs for the c-*Myc* promoter predicted by PROMO and UCSC databases. D, The interaction strength between *SNHG17* and c-Jun was predicted using the catRAPID algorithm (http://s.tartaglialab.com/page/catrapid_group). E, CatRAPID fragment module prediction of the interaction profile between c-Jun protein and *SNHG17*. F, Whole cell lysates and nuclear fraction were incubated with in vitro transcribed RNA of sense (S) and antisense (AS) *SNHG17*. Validation of *SNHG17* and c-Jun interaction by RNA pull down. G, RIP assays verified the direct interaction of *SNHG17* with c-Jun. IgG antibody served as the negative control. H, Lack of the c-Jun-binding domain in *SNHG17* involving the truncation mutants. Immunoblot analysis for c-Jun in protein samples pulled down by full-length *SNHG17* and the *SNHG17* truncated mutant (Δ101-400). *GAPDH* was used as a negative RNA control. I, Immunoblot of His-tagged c-Jun (WT vs domain truncation mutants) retrieved by biotinylated SNHG17; the structure of c-Jun is shown below. The data are shown as mean ± SD, $^{**}P < .01$

its expression following TGFβ1 treatment in Eca109 cells (Figure 3A). The expression of Eca was significantly downregulated, while the levels of N-cadherin, Twist1, and SNAI2 expression in Eca109 cells was increased following TGF-β1 treatment (Figure 3B). As *SNHG17* was induced by TGF-β1, we further investigated whether silencing *SNHG17* abrogated TGF-β-mediated EMT. As shown in Figure 3C, TGF-β-induced EMT in Eca109 cells produced an epithelial-to-mesenchymal signature. The cells treated with TGF-β1 changed their original cobble-stone shape to a spindle-like shape, while depletion of *SNHG17* prominently restrained the spindle-like formation. In addition, downregulation of *SNHG17* largely overrode the TGF-β treatment suppressed E-cadherin and induced the expression of N-cadherin, Twist1, and SNAI2 in *SNHG17*-deficient cells (Figure 3D,E). Taken together, these data indicated that *SNHG17* may be an EMT-related lncRNA and contribute to TGF-β-induced EMT in ESCC cells.

3.4 | *SNHG17* upregulates the expression of c-Myc and medicates the PI3K/AKT pathway in ESCC

To elucidate the potential mechanism by which *SNHG17* promotes the progression of ESCC, we performed an RNA-sequencing assay

after Eca109 cells were transfected with *shSNHG17*. In total, 215 protein-coding genes were upregulated, while 145 were downregulated. Based on the Kyoto Encyclopedia of Genes and Genomes (KEGG) database pathway enrichment analysis and Gene Ontology terms of all essential genes, these data suggested that most genes in the PI3K/Akt signaling pathway were enriched and related to the proliferation and migration of cells (Figures 4A and S3). Among these, the top 5 genes were c-*Myc*, *CLDN4*, *IL7R*, *JAK3*, and *AREG*, and their

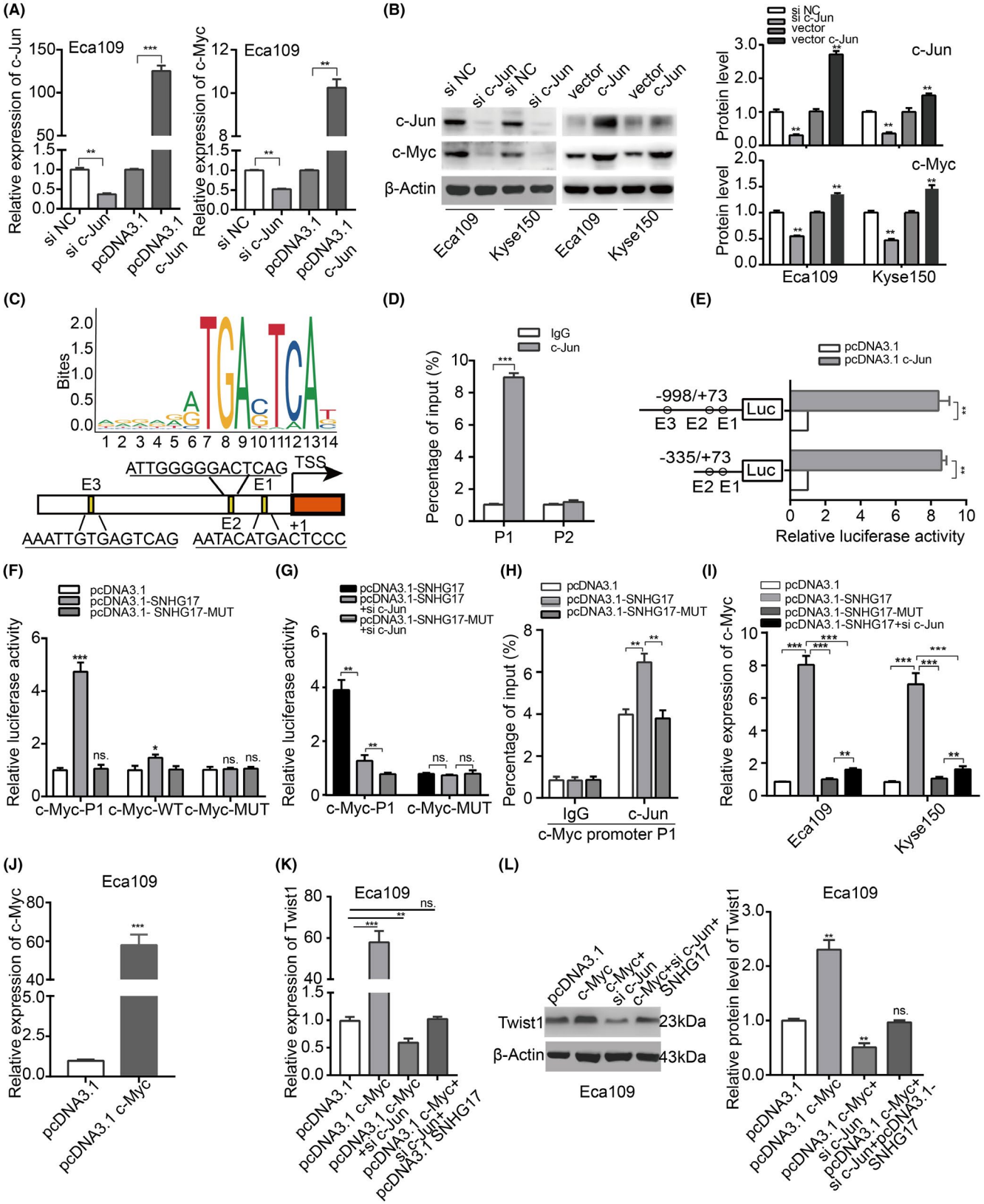

FIGURE 6 *SNHG17* recruits c-Jun, which regulates the expression of c-Myc by binding to its promoter region. A, qRT-PCR for mRNA levels of c-*Jun* and c-*Myc* in the transfection of Eca109 and Kyse150 cells. B, Western blot assays for protein levels of c-Jun and c-Myc in transfected Eca109 and Kyse150 cells. C, Predicted c-Jun binding site in the −1000 bp region of the c-*Myc* promoter using JASPAR (E1: −17 to −30 bp; E2: −103 to −116 bp; and E3: −757 to 770 bp). D, ChIP-qPCR assays were conducted to show direct binding between c-Jun and c-*Myc* promoter regions in Eca109 (the P1 region contained E1 and E2 sites, the P2 region contained the E3 site). E, Verified c-*Myc* promoter sequences were added into a pGL3 vector. The activity of the c-*Myc* promoter containing or lacking c-Jun-binding elements was detected as luciferase reporter assays. F, G, Interaction between *SNHG17*, c-Jun, and c-Myc was confirmed by luciferase reporter assays. H, ChIP-qPCR analysis revealed that *SNHG17* fortified the enrichment of c-Jun in the c-*Myc* promoter through the region of *SNHG17* binding to c-Jun. IgG was the normalized control for qRT-PCR analysis. I, Expression of c-*Myc* was measured by qRT-PCR assay in *SNHG17*, SNHG17-MUT, or si c-*Jun* and *SNHG17* co-transfected Eca109 and Kyse150 cells. J, qRT-PCR for mRNA levels of c-*Myc* in the transfection of Eca109 cells. K, L, qRT-PCR and western blot assays showed the expression of Twist1 in the different groups of Eca109 cells of overexpressing c-*Myc*/c-*Myc* + si c-*Jun*/c-*Myc* + si c-*Jun* + *SNHG17*. Data are shown as the mean ± SD, $^{**}P < .01$, $^{***}P < .001$

regulation under *SNHG17* silencing or overexpression was evaluated by qRT-PCR. The data showed that the level of c-*Myc* mRNA was decreased with knockdown of *SNHG17*, but increased with ectopic upregulation of *SNHG17* (Figure 4B). Moreover, expression of c-*Myc* mRNA was positively correlated with *SNHG17* expression in 128 cases of ESCC tissues (Figure 4C). Additionally, the expression of c-Myc, p-PI3K and p-AKT proteins was downregulated with the knockdown of *SNHG17*, whereas protein expression was dramatically upregulated with the ectopic expression of *SNHG17* (Figure 4D). c-Myc was confirmed to having a prominent role in sustaining tumor growth in many tumor types, including ESCC.[26] As shown by ISH and IHC, we found that tumor samples for high expression of *SNHG17* showed an increased expression frequency of c-Myc protein, and positive staining occurred in the nucleus (Figure 4E). Therefore, we speculated that *SNHG17* positively regulated c-Myc expression.

3.5 | *SNHG17* binds to transcription factor c-Jun

The dysregulation of *SNHG17* decreased the expression of c-Myc dramatically. Furthermore, overexpression of *SNHG17* increased the transcriptional activity of the c-*Myc* promotor, indicating that *SNHG17* potentially regulated c-Myc by acting on its promoter (Figure 5A). Subsequently, to explore the molecular mechanism by which *SNHG17* modulates c-Myc expression, we further examined the localization of *SNHG17* through subcellular fractionation in Eca109 and Kyse150 cells, illustrating that *SNHG17* was predominantly localized in the nucleus (Figure 5B). According to a previous study, lncRNAs located in the nucleus regulated the transcriptional process through binding to transcription factors (TFs), which in turn degenerated the DNA sequence motifs on the promoter in specific oncogenes in cancer cells.[27] Therefore, we proposed a tentative mechanism in which SNHG17/TF may activate c-Myc expression through binding to the promoter region. First, we predicted the TF binding to the c-*Myc* promoter region using PROMO and University of California, Santa Cruz (UCSC) genome browser (Figure 5C). Then, we evaluated the possibility of *SNHG17* interaction with the TFs via the catRAPID algorithm. Notably, the interaction between *SNHG17* and c-Jun was higher (Figures 5D and S4A,B). CatRAPID fragments was used to estimate individual interaction propensities of polypeptide and nucleotide sequence fragments, further suggesting that the 100-400 nucleotide positions of the *SNHG17* sequence may bind to the amino acid residues of the c-Jun protein with high propensity (Figure 5E). c-Jun is also a TF that regulates TGF-β1 at the transcriptional level.[28] We also found that depletion of c-Jun attenuated the ectopic expression of *SNHG17* induced by TGF-β1 (Figure S4C). Therefore, TF c-Jun was selected for further research.

To evaluate the interaction between *SNHG17* and c-Jun, both whole cell lysate and nuclear fraction were incubated with biotinylated *SNHG17* or its antisense RNA transcribed in vitro, the results of the RNA pull-down assay revealed that *SNHG17* bound to c-Jun mainly in the nucleus. Reciprocally, a c-Jun RIP assay was performed, and further showed that *SNHG17* was enriched in the anti-c-Jun immunoprecipitation in Eca109 and Kyse150 cells (Figure 5F,G).

To further map the specific region of *SNHG17*/c-Jun interaction, deletion mutants of *SNHG17* were constructed. Deletion mapping analysis identified that the 100-400 nucleotide region was required for *SNHG17* interaction with c-Jun. To further examine which motif of c-Jun interacts with *SNHG17*, a truncated c-Jun was applied according to the protein domain; this showed that His-tagged c-Jun-truncated mutant (Δ243-331aa) was more critical for c-Jun-*SNHG17* binding (Figure 5H,I). However, we also found the expression of c-Jun was not altered by *SNHG17* knockdown, suggesting that *SNHG17* does not participate in the regulation of c-Jun (Figure S4D).

3.6 | *SNHG17* recruits c-Jun, which regulates the expression of c-*Myc* by binding its promoter region

Next, we analyzed the effect of c-Jun on c-Myc in ESCC cells. First, we concluded that the knockdown of c-Jun reduced, while the overexpression induced, the level of c-*Myc* mRNA and protein (Figure 6A,B). Consistently, c-Myc overexpression partially reversed the inhibition of c-Jun knockdown on the proliferation, migration, and invasion of esophageal cancer cells (Figure S5). JASPAR CORE database was used to predict the binding sites of c-Jun in the c-*Myc* promoter; 3 potential positions were identified (Figure 6C). To further explore whether c-Jun directly bound to the c-*Myc* promoter, we found by ChIP assay that c-Jun was enriched in the region of the c-*Myc* promoter (Figure 6D). Importantly, overexpression of c-Jun

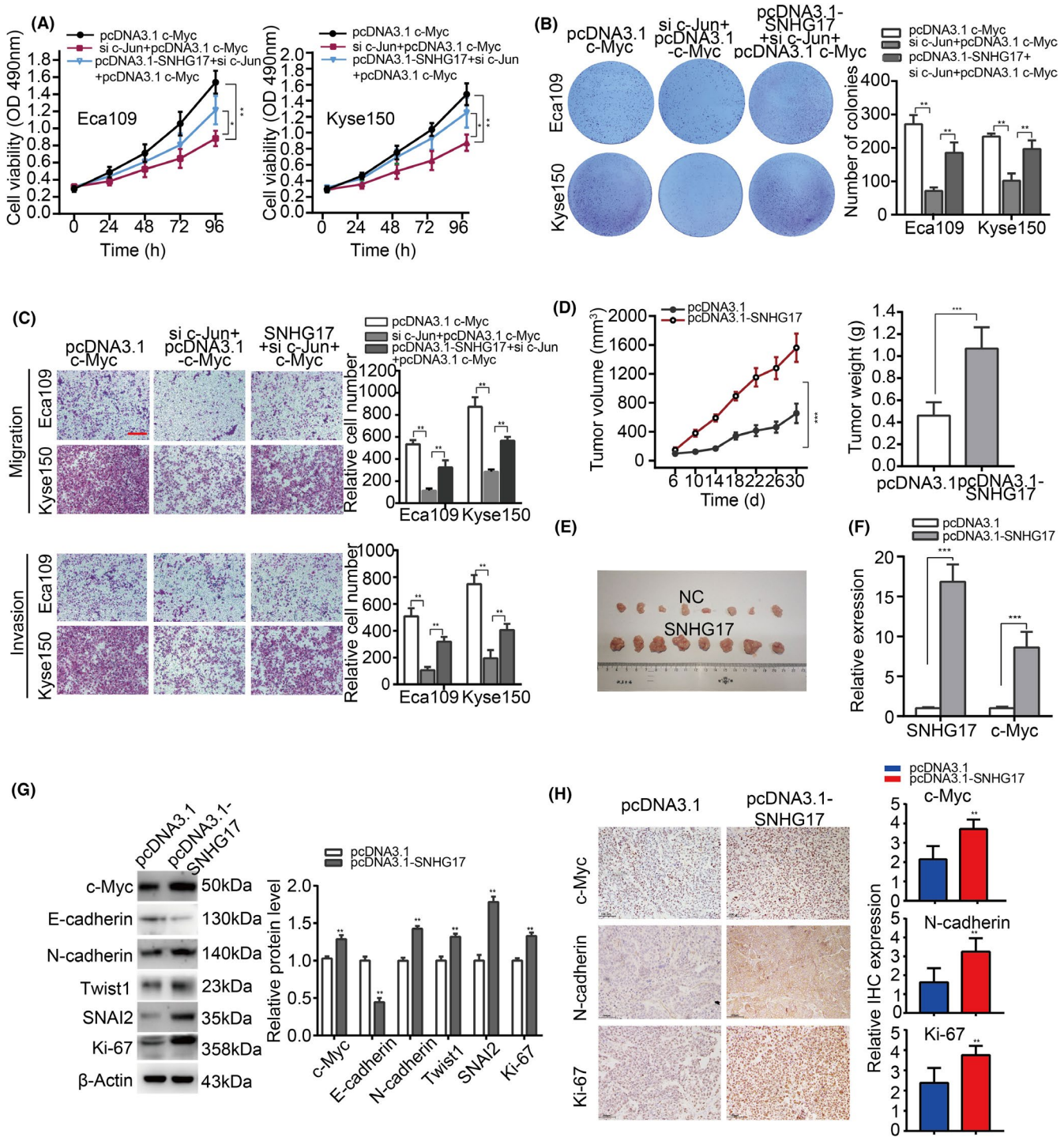

FIGURE 7 *SNHG17*/c-Jun/c-Myc axis promotes ESCC cells growth and metastasis in vitro and in vivo. A, B, MTS and colony formation assays were performed to examine the effect of the *SNHG17*/c-Jun/c-Myc axis on cell proliferation ability of Eca109 and Kyse150 cells. C, Transwell assay was performed for evaluating the effect of the *SNHG17*/c-Jun/c-Myc axis on cell invasion and metastatic ability of Eca109 and Kyse150 cells in each group. D, E, Eca109 cells stably overexpressing *SNHG17* were subcutaneously injected into nude mice and xenografts. The growth curve and final tumor weight of xenografts from mice in groups with different treatments (n = 8). F, qRT-PCR analysis showed that the expression of *SNHG17* and c-Myc in xenograft tissues with overexpression of *SNHG17*. G, Western blot assays were performed to measure c-Myc, E-cadherin, N-cadherin, Twist1, SNAI2, and Ki67 expression levels in xenografts of mice with different treatments. H, IHC staining of c-Myc, N-cadherin, and Ki-67 in the xenografts of mice in the 2 groups. The results are shown as the mean ± SD. ***$P < .001$

markedly accelerated the c-*Myc* promoter activity in Eca109 cells but only in the presence of the vector containing the c-*Myc* promoter E1/E2 (Figure 6E).

Based on the above data that *SNHG17* could bind to c-Jun, we further verified whether *SNHG17* recruits c-Jun to bind within the region of the c-*Myc* promoter. An *SNHG17*- truncated mutant (SNHG17-MUT) (Δ101-400 bp) was created and co-transfected with the pGL3-c-Myc promoter, the results demonstrated that SNHG17-MUT or lack of c-Jun-binding motifs had no effect on the activity of c-Myc transcription, while *SNHG17* fortified the transcription activity of the c-*Myc* promotor. The potentiation of *SNHG17* upregulation on the activity of c-Myc transcription could be attenuated by a c-Jun reduction (Figure 6F,G). Moreover, ChIP assay further revealed that *SNHG17* overexpression could increase the enrichment of c-Jun on the c-*Myc* promoter, while overexpression of SNHG17-MUT did not influence the binding ability of c-Jun to the c-*Myc* promoter (Figure 6H). In contrast with *SNHG17* or SNHG17-MUT, transfection of pcDNA3.1-SNHG17 + si c-Jun significantly reduced the effect of *SNHG17* on c-Myc expression. (Figure 6I). According to previous publications, Twist1 is a direct transcriptional target of c-Myc in cancer.[29] To assess that the expression promoting effect of c-Myc on Twist1, a pcDNA3.1 c-Myc plasmid was constructed and transfected into Eca109 cells. Then, qRT-PCR and western blotting assays were conducted to reveal that the expression of Twist1 was upregulated by the plasmid in pcDNA3.1 c-Myc. Nevertheless, upregulation of Twis1 was restored under conditions of low c-Jun expression, overexpressing c-Myc. While, *SNHG17* overexpression could partly rescue the negative effect of de-regulation of c-Jun on Twist1 expression (Figure 6J-L). Overall, *SNHG17* recruited c-Jun to promote c-Myc transcription and Twist1 transcription, which resulted in ESCC EMT.

3.7 | *SNHG17*/c-Jun/c-Myc axis promotes ESCC cell growth and metastasis in vitro and in vivo

Rescue assays were performed to observe whether *SNHG17* boosted ESCC progression through the regulation of c-Myc, and whether c-Jun reduced the effect of *SNHG17* on the c-Myc expression. The results showed that transfection of pcDNA3.1-SNHG17 + si c-Jun + pcDNA3.1c-Myc could partially reverse the inhibition of si c-Jun + pcDNA3.1c-Myc on the proliferation, migration, and invasion of esophageal cancer cells (Figure 7A-C).

Next, we performed tumor xenograft experiments to further investigate the effects of *SNHG17* on tumor growth in vivo. In total, 1×10^7 Eca109 cells with stable expression of *SNHG17* or control cells were injected subcutaneously into BALB/c nude mice. The tumors formed by SNHG17-upregulated xenografts increased in nude mice compared with those in the control group, and the tumor volume and weight were monitored (Figure 7D,E). Also, qRT-PCR analysis showed that overexpression of *SNHG17* increased the expression of *SNHG17* and c-Myc in xenograft tissues (Figure 7F). To further elucidate the tumorigenic ability of *SNHG17*, the data of western blot indicated that the levels of c-Myc, N-cadherin, Twist1, SNAI2, and Ki-67 were enhanced by *SNHG17* upregulation in xenografts (Figure 7G). Consistently, IHC assay showed that the xenograft tissues formed by *SNHG17* upregulation showed higher positive staining for c-Myc, N-cadherin and Ki-67 than that in the control group (Figure 7H). Together, these findings suggested that *SNHG17* facilitates ESCC tumor growth in vivo.

4 | DISCUSSION

In the present study, we confirmed that *SNHG17* was upregulated in ESCC tissues and cell lines and was a poor prognosis factor for ESCC patients. Next, functional assays showed that *SNHG17* promotes ESCC cell proliferation, migration, and invasion, and restricts cell apoptosis. Furthermore, *SNHG17* was required for TGF-β-induced EMT; it directly triggered c-Myc expression by recruiting TF c-Jun in ESCC progression. These findings potentially provided a new perspective to boost treatment efficacy and improve prognosis in ESCC patients.

Reportedly, *SNHG17* functions as a cancer-associated lncRNA are linked to diverse diseases.[23,30] Previously, Xu et al[16] explained that upregulated *SNHG17* promotes the proliferation and migration in non–small-cell lung cancer. Wu et al[14] showed that *SNHG17* aggravates prostate cancer progression via regulation of the homolog SNORA71B. In ovarian cancer,[31] *SNHG17* was deemed as an oncogene, which regulated the expression of CDK6 by acting as a molecular sponge for miR-214-3p. Accumulating evidence showed that *SNHG17* exerts its regulatory role predominantly in the cytoplasm. In the current study, we verified that *SNHG17* was predominantly located in the nucleus, as revealed by the cellular fractionation assay. This finding was consistent with the results from the study by Zhang et al.[22] In the nucleus, lncRNAs mainly participate in tumorigenesis and progression at the epigenetic and transcriptional level. Liu et al[32] demonstrated that SNHG12 located in the nucleus and upregulates CDCA3 by stabilizing the transcription factor SP1. In addition, SNHG15 promoted colon cancer progression through binding and maintaining Slug stability.[33] Here, we assumed that, in the nucleus, *SNHG17* might act as a transcription co-activator regulating the target genes at the transcriptional level. Here, RIP and RNA-pulldown assays illustrated that *SNHG17* is directly bound to c-Jun in ESCC cells, which was different from that in the previous studies on the molecular mechanism of *SNHG17* regulation. Furthermore, the study showed that the aberrant activation of c-Jun played a key role in regulating cellular invasion.[34] This phenomenon could be activated or restrained by various types of modifications, such as phosphorylation or glycosylation.[35,36] Xu et al[37] clarified that SNHG1 induced MMP2 transcription via boosting c-Jun protein phosphorylation. Furthermore, we assumed that *SNHG17* upregulation stabilized the c-Jun protein. ChIP assays determined that *SNHG17* synchronously recruited c-Jun to c-*Myc* promoter regions and repressed transcription.

EMT is characterized by epithelial cells acquiring the mesenchymal cell phenotype, which is widely implicated in tumor invasion and metastasis. TGF-β, a potent EMT-inducing cytokine, promotes cancer cell invasion and metastasis.[38-40] Previous studies have indicated that TGF-β induced several lncRNAs, such as lncRNA-ELIT-1,[41] lncRNA-smad7,[42] lncRNA UCA1,[43] lncRNA-ATB,[44] lncRNA NKILA,[45] MALAT1,[46] and MEG3,[47] which are crucial for carcinogenic processes orchestrated by TGF-β. lncRNA-ELIT-1, lincRNA-ATB, lncRNA NKILA, MALAT1, and MEG3 are involved in EMT. In the current study, *SNHG17* expression was upregulated by TGF-β1 treatment in Eca109 cells, which created an effect on EMT, including E-cadherin and N-cadherin. Furthermore, we found that depletion of *SNHG17* prominently restrained the original cobble-stone shape to a spindle-like shape, spindle-like formation in Eca109 cell lines, and its depletion also largely overrode the inhibition of E-cadherin and the induction of N-cadherin by TGF-β treatment. Therefore, *SNHG17* was deemed to be an EMT-related lncRNA and positively contributed to TGF-β-induced EMT in ESCC cells.

c-Myc is a vital tumor promoter, and its expression can be controlled by lncRNAs at the transcriptional and post-transcriptional levels.[26] In previous findings, lncRNA PVT1, linc-ROR, and lncRNA CCAT1-L aggravated tumorigenesis and participated in c-Myc-dependent EMT.[48-50] Moreover, Bhowmick et al[51] highlighted that TGF-β rapidly activates RhoA to promote the EMT procession of breast cancer, indicating that TGF-β-mediated EMT was independent of SMAD signaling. Grille et al[52] showed that EMT was activated by AKT in the HSCC cell line SCC15. This study provided an insight into the oncogenic function of *SNHG17*, which is partially dependent on c-Myc to exert a carcinogenic effect through rescue experiments. Furthermore, TGF-β-induced *SNHG17* boosts protein expression of c-Myc, p-PI3K, and p-AKT. In addition, previous studies have confirmed that Twist1 acted a direct transcriptional target of Myc in cancer cells, and Twist1 elicited metastasis of MYC related-HCC.[29,53] In the present study, we indicated that *SNHG17* acted as an EMT-related lncRNA through TGF-β1 regulation to promote the expression of c-Myc and Twist1. Overexpression of *SNHG17* and knocking down c-*Jun* could partially reverse the inhibition of c-*Jun* knock down on the migration and invasion of esophageal cancer cells. Therefore, we assumed that *SNHG17* aggravated EMT progression via the *SNHG17*/c-Jun/c-Myc/Twist1 axis in ESCC.

Taken together, the present study demonstrated that TGF-β1-induced *SNHG17* accelerated malignancy in ESCC. Additionally, *SNHG17* stimulated the EMT process and exerted the oncogenic function depending on c-Myc by recruiting c-Jun to enhance c-Myc expression and Twist1. As an upstream TF of TGF-β1, c-Jun regulates TGF-β1 at the transcriptional level.[28] This phenomenon indicated that *SNHG17*-recruited c-Jun triggers TGF-β1-induced *SNHG17*. Moreover, the data provided a novel therapeutic perspective by targeting oncogenic *SNHG17* in ESCC. Strikingly, the molecular mechanism of *SNHG17* is considered as the entry point for further screening the targets of drugs antagonistic in in vivo and in vitro experiments for ESCC.

ACKNOWLEDGMENTS

This study was supported by Grants from the National Natural Science Foundation (Nos. 81472335, 81772612). Natural Science Foundation of Hebei Province, China (No. H2019206664) and the Department of Education of Hebei Province (No. CXZZBS2020115).

DISCLOSURE

The authors declare no potential conflicts of interest.

ORCID

Wei Guo https://orcid.org/0000-0001-9690-161X
Zhiming Dong https://orcid.org/0000-0002-7884-935X

REFERENCES

1. Bray F, Ferlay J, Soerjomataram I, Siegel RL, Torre LA, Jemal A. Global cancer statistics 2018: GLOBOCAN estimates of incidence and mortality worldwide for 36 cancers in 185 countries. *CA Cancer J Clin*. 2018;68:394-424.
2. Fatehi HA, Chehade R, Breadner D, Raphael J. Esophageal carcinoma: towards targeted therapies. *Cell Oncol*. 2020;43:195-209.
3. Guohong Z, Min SU, DuenMei W, et al. Genetic heterogeneity of oesophageal cancer in high-incidence areas of southern and northern China. *PLoS One*. 2010;5:e9668.
4. Torre LA, Bray F, Siegel RL, Ferlay J, Lortet-Tieulent J, Jemal A. Global cancer statistics, 2012. *CA Cancer J Clin*. 2015;65:87-108.
5. Pennathur A, Gibson MK, Jobe BA, Luketich JD. Oesophageal carcinoma. *Lancet*. 2013;381:400-412.
6. Zeng H, Chen W, Zheng R, et al. Changing cancer survival in China during 2003–15: a pooled analysis of 17 population-based cancer registries. *Lancet Glob Health*. 2018;6:e555-e567.
7. Guttman M, Amit I, Garber M, et al. Chromatin signature reveals over a thousand highly conserved large non-coding RNAs in mammals. *Nature*. 2009;458:223-227.
8. Stein LD. Human genome: end of the beginning. *Nature*. 2004;431:915-916.
9. Chew CL, Conos SA, Unal B, Tergaonkar V. Noncoding RNAs: master regulators of inflammatory signaling. *Trends Mol Med*. 2018;24:66-84.
10. Yao RW, Wang Y, Chen LL. Cellular functions of long noncoding RNAs. *Nat Cell Biol*. 2019;21:542-551.
11. Goodall GJ, Wickramasinghe VO. RNA in cancer. *Nat Rev Cancer*. 2020;21(1):22-36.
12. Schmitt AM, Chang HY. Long noncoding RNAs in cancer pathways. *Cancer Cell*. 2016;29:452-463.
13. Liu JX, Li W, Li JT, Liu F, Zhou L. Screening key long non-coding RNAs in early-stage colon adenocarcinoma by RNA-sequencing. *Epigenomics*. 2018;10:1215-1228.
14. Wu G, Hao C, Qi X, et al. LncRNA SNHG17 aggravated prostate cancer progression through regulating its homolog SNORA71B via a positive feedback loop. *Cell Death Dis*. 2020;11:393.
15. Han T, Jing X, Bao J, et al. *H pylori* infection alters repair of DNA double-strand breaks via SNHG17. *J Clin Invest*. 2020;130:3901-3918.
16. Xu T, Yan S, Jiang L, et al. Gene amplification-driven long non-coding RNA SNHG17 regulates cell proliferation and migration in human non-small-cell lung cancer. *Mol Ther Nucleic Acids*. 2019;17:405-413.
17. Bakir B, Chiarella AM, Pitarresi JR, Rustgi AK. EMT, MET, plasticity, and tumor metastasis. *Trends Cell Biol*. 2020;30:764-776.
18. Li J, Li Z, Zheng W, et al. LncRNA-ATB: an indispensable cancer-related long noncoding RNA. *Cell Prolif*. 2017;50:e12381.
19. Yuan JH, Yang F, Wang F, et al. A long noncoding RNA activated by TGF-beta promotes the invasion-metastasis cascade in hepatocellular carcinoma. *Cancer Cell*. 2014;25(5):666-681.

20. Yang C, Li X, Wang Y, Zhao L, Chen W. Long non-coding RNA UCA1 regulated cell cycle distribution via CREB through PI3-K dependent pathway in bladder carcinoma cells. *Gene*. 2012;496:8-16.
21. Tong F, Guo J, Miao Z, Li Z. LncRNA SNHG17 promotes the progression of oral squamous cell carcinoma by modulating miR-375/PAX6 axis. *Cancer Biomark*. 2020;30(1):1-12.
22. Zhang G, Xu Y, Wang S, et al. LncRNA SNHG17 promotes gastric cancer progression by epigenetically silencing of p15 and p57. *J Cell Physiol*. 2019;234:5163-5174.
23. Liu Y, Li Q, Tang D, et al. SNHG17 promotes the proliferation and migration of colorectal adenocarcinoma cells by modulating CXCL12-mediated angiogenesis. *Cancer Cell Int*. 2020;20:566.
24. Alam KJ, Mo J-S, Han S-H, et al. MicroRNA 375 regulates proliferation and migration of colon cancer cells by suppressing the CTGF-EGFR signaling pathway. *Int J Cancer*. 2017;141:1614-1629.
25. Ros M, Sala M, Saltel F. Linking matrix rigidity with EMT and cancer invasion. *Dev Cell*. 2020;54:293-295.
26. Yu VZ, Ko JMY, Ning L, Dai W, Law S, Lung ML. Endoplasmic reticulum-localized ECM1b suppresses tumor growth and regulates MYC and MTORC1 through modulating MTORC2 activation in esophageal squamous cell carcinoma. *Cancer Lett*. 2019;461:56-64.
27. Long Y, Wang X, Youmans DT, Cech TR. How do lncRNAs regulate transcription? *Sci Adv*. 2017;3:eaao2110.
28. Gao SL, Yin R, Zhang LF, et al. The oncogenic role of MUC12 in RCC progression depends on c-Jun/TGF-beta signalling. *J Cell Mol Med*. 2020;24:8789-8802.
29. Selmi A, de Saint-Jean M, Jallas A-C, et al. TWIST1 is a direct transcriptional target of MYCN and MYC in neuroblastoma. *Cancer Lett*. 2015;357:412-418.
30. Li H, Li T, Huang D, Zhang P. Long noncoding RNA SNHG17 induced by YY1 facilitates the glioma progression through targeting miR-506-3p/CTNNB1 axis to activate Wnt/beta-catenin signaling pathway. *Cancer Cell Int*. 2020;20:29.
31. Pan X, Guo Z, Chen Y, et al. STAT3-induced lncRNA SNHG17 exerts oncogenic effects on ovarian cancer through regulating CDK6. *Mol Ther Nucleic Acids*. 2020;22:38-49.
32. Liu Y, Cheng G, Huang Z, et al. Long noncoding RNA SNHG12 promotes tumour progression and sunitinib resistance by upregulating CDCA3 in renal cell carcinoma. *Cell Death Dis*. 2020;11:515.
33. Jiang H, Li T, Qu YI, et al. Long non-coding RNA SNHG15 interacts with and stabilizes transcription factor Slug and promotes colon cancer progression. *Cancer Lett*. 2018;425:78-87.
34. Bao M-H, Lv Q-L, Szeto V, et al. TRPM2-AS inhibits the growth, migration, and invasion of gliomas through JNK, c-Jun, and RGS4. *J Cell Physiol*. 2020;235:4594-4604.
35. Priyadarshini R, Hussain M, Attri P, et al. BLM potentiates c-jun degradation and alters its function as an oncogenic transcription factor. *Cell Rep*. 2018;24:947-961.e7.
36. Sundqvist A, Voytyuk O, Hamdi M, et al. JNK-dependent cJun phosphorylation mitigates TGFbeta- and EGF-induced pre-malignant breast cancer cell invasion by suppressing AP-1-mediated transcriptional responses. *Cells*. 2019;8:1481.
37. Xu J, Yang R, Hua X, et al. lncRNA SNHG1 promotes basal bladder cancer invasion via interaction with PP2A catalytic subunit and induction of autophagy. *Mol Ther Nucleic Acids*. 2020;21:354-366.
38. Wang J, Shao N, Ding X, et al. Crosstalk between transforming growth factor-beta signaling pathway and long non-coding RNAs in cancer. *Cancer Lett*. 2016;370:296-301.
39. Lamouille S, Xu J, Derynck R. Molecular mechanisms of epithelial-mesenchymal transition. *Nat Rev Mol Cell Biol*. 2014;15:178-196.
40. Chen Z, He S, Zhan Y, et al. TGF-beta-induced transgelin promotes bladder cancer metastasis by regulating epithelial-mesenchymal transition and invadopodia formation. *EBioMedicine*. 2019;47:208-220.
41. Sakai S, Ohhata T, Kitagawa K, et al. Long noncoding RNA ELIT-1 acts as a Smad3 cofactor to facilitate TGFbeta/Smad signaling and promote epithelial-mesenchymal transition. *Cancer Res*. 2019;79:2821-2838.
42. Arase M, Horiguchi K, Ehata S, et al. Transforming growth factor-beta-induced lncRNA-Smad7 inhibits apoptosis of mouse breast cancer JygMC(A) cells. *Cancer Sci*. 2014;105(8):974-982.
43. Zhang Y, Fan K, Xu X, Wang A. The TGF-beta1 induces the endothelial-to-mesenchymal transition via the UCA1/miR-455/ZEB1 regulatory axis in human umbilical vein endothelial cells. *DNA Cell Biol*. 2020;39:1264-1273.
44. Tang F, Wang H, Chen E, et al. LncRNA-ATB promotes TGF-beta-induced glioma cells invasion through NF-kappaB and P38/MAPK pathway. *J Cell Physiol*. 2019;234:23302-23314.
45. Wu W, Chen F, Cui X, et al. LncRNA NKILA suppresses TGF-beta-induced epithelial-mesenchymal transition by blocking NF-kappaB signaling in breast cancer. *Int J Cancer*. 2018;143:2213-2224.
46. Yang S, Yao H, Li M, Li H, Wang F. Long non-coding RNA MALAT1 mediates transforming growth factor Beta1-induced epithelial-mesenchymal transition of retinal pigment epithelial cells. *PLoS One*. 2016;11:e0152687.
47. Mondal T, Subhash S, Vaid R, et al. MEG3 long noncoding RNA regulates the TGF-beta pathway genes through formation of RNA-DNA triplex structures. *Nat Commun*. 2015;6:7743.
48. Riquelme E, Suraokar MB, Rodriguez J, et al. Frequent coamplification and cooperation between C-MYC and PVT1 oncogenes promote malignant pleural mesothelioma. *J Thorac Oncol*. 2014;9:998-1007.
49. Xiang J-F, Yin Q-F, Chen T, et al. Human colorectal cancer-specific CCAT1-L lncRNA regulates long-range chromatin interactions at the MYC locus. *Cell Res*. 2014;24:513-531.
50. Huang J, Zhang A, Ho T-T, et al. Linc-RoR promotes c-Myc expression through hnRNP I and AUF1. *Nucleic Acids Res*. 2016;44:3059-3069.
51. Bhowmick NA, Ghiassi M, Bakin A, et al. Transforming growth factor-beta1 mediates epithelial to mesenchymal transdifferentiation through a RhoA-dependent mechanism. *Mol Biol Cell*. 2001;12:27-36.
52. Grille SJ, Bellacosa A, Upson J, et al. The protein kinase Akt induces epithelial mesenchymal transition and promotes enhanced motility and invasiveness of squamous cell carcinoma lines. *Cancer Res*. 2003;63:2172-2178.
53. Dhanasekaran R, Baylot V, Kim M, et al. MYC and Twist1 cooperate to drive metastasis by eliciting crosstalk between cancer and innate immunity. *eLife*. 2020;9:e50731.

SUPPORTING INFORMATION

Additional supporting information may be found in the online version of the article at the publisher's website.

How to cite this article: Shen S, Liang J, Liang X, et al. *SNHG17*, as an EMT-related lncRNA, promotes the expression of c-Myc by binding to c-Jun in esophageal squamous cell carcinoma. *Cancer Sci*. 2022;113:319–333. https://doi.org/10.1111/cas.15184